

JGR Biogeosciences

RESEARCH ARTICLE

10.1029/2019JG005266

This article is a companion to Phillips,
<https://doi.org/10.1029/2020JG005668>.

Key Points:

- Soil warming over the 21st century keeps pace with air warming in tropical and snow-free regions but lags air warming in colder regions
- Air warming is not a good proxy for soil warming in regions where snow and ice impede transfer of sensible heat from the atmosphere to soil
- Deep (100 cm) and near-surface (~1 cm) soil layers warm at the same rate across all soil orders globally

Supporting Information:

- Supporting Information S1

Correspondence to:

J. L. Soong,
jsoong@lbl.org

Citation:

Soong, J. L., Phillips, C. L., Ledna, C., Koven, C. D., & Torn, M. S. (2020). CMIP5 models predict rapid and deep soil warming over the 21st century. *Journal of Geophysical Research: Biogeosciences*, 125, e2019JG005266. <https://doi.org/10.1029/2019JG005266>

Received 21 MAY 2019

Accepted 27 DEC 2019

Accepted article online 5 JAN 2020

Author Contributions:

Conceptualization: Claire L. Phillips, Charles D. Koven, Margaret S. Torn

Data curation: Claire L. Phillips, Catherine Ledna

Formal analysis: Jennifer L. Soong, Claire L. Phillips, Catherine Ledna, Charles D. Koven

Funding acquisition: Margaret S. Torn
(continued)

© 2020. The Authors.

This is an open access article under the terms of the Creative Commons Attribution-NonCommercial-NoDerivs License, which permits use and distribution in any medium, provided the original work is properly cited, the use is non-commercial and no modifications or adaptations are made.

CMIP5 Models Predict Rapid and Deep Soil Warming Over the 21st Century

Jennifer L. Soong¹, Claire L. Phillips², Catherine Ledna³, Charles D. Koven¹, and Margaret S. Torn¹

¹Lawrence Berkeley National Laboratory, Climate and Ecosystem Sciences Division, Berkeley, CA, USA, ²Forage Seed and Cereal Research Unit, USDA-ARS, Corvallis, OR, USA, ³Energy Resources Group, University of California at Berkeley, Berkeley, CA, USA

Abstract Despite the fundamental importance of soil temperature for Earth's carbon and energy budgets, ecosystem functioning, and agricultural production, studies of climate change impacts on soil processes have mainly relied on air temperatures, assuming they are accurate proxies for soil temperatures. We evaluated changes in soil temperature, moisture, and air temperature predicted over the 21st century from 14 Earth system models. The model ensemble predicted a global mean soil warming of 2.3 ± 0.7 and 4.5 ± 1.1 °C at 100-cm depth by the end of the 21st century for RCPs 4.5 and 8.5, respectively. Soils at 100 cm warmed at almost exactly the same rate as near-surface (~1 cm) soils. Globally, soil warming was slightly slower than air warming above it, and this difference increased over the 21st century. Regionally, soil warming kept pace with air warming in tropical and arid regions but lagged air warming in colder regions. Thus, air warming is not necessarily a good proxy for soil warming in cold regions where snow and ice impede the direct transfer of sensible heat from the atmosphere to soil. Despite this effect, high-latitude soils were still projected to warm faster than elsewhere, albeit at slower rates than surface air above them. When compared with observations, the models were able to capture soil thermal dynamics in most biomes, but some failed to recreate thermal properties in permafrost regions. Particularly in cold regions, using soil warming rather than air warming projections may improve predictions of temperature-sensitive soil processes.

1. Introduction

Temperature is critical for agricultural production (FAO, 1985) and carbon exchange between terrestrial ecosystems and the atmosphere, including soil carbon storage and soil respiration (Davidson & Janssens, 2006). Despite the sensitivity of many soil processes to temperature, the effect of global warming on soil temperatures per se has received little attention. This reflects in part the implicit assumption that the relationship between mean annual soil temperatures and mean annual air temperatures, developed under quasi steady state conditions, will persist under conditions of rapid climate change (Schmidt et al., 2001; Smerdon et al., 2003). While air temperature data are important for characterizing a wide number of climate-sensitive processes, including optimal climate zones and growing periods for plant growth (USDA, 1994), soil temperature directly influences many key belowground plant growth factors such as germination and early season crop emergence (Chen et al., 2007), root growth (FAO, 1985; Kaspar & Bland, 1992), soil water uptake (Wraith & Ferguson, 1994), the viability of some crop damaging pests (Huang, 2016), and release of soil carbon and greenhouse gases to the atmosphere (Hicks Pries et al., 2017). Thus, it is critical to understand how soil temperatures will change over the next century and whether air temperature can be used as a proxy for soil temperatures under rapid climate change.

Soil and whole ecosystem impacts are more commonly linked to warming air temperatures than to soil warming likely due to the greater prevalence of air temperature data. However, more data on long-term soil temperature trends are becoming available. Data analyses from the United States (Hao et al., 2014; Hu & Feng, 2003; Mohler & Harrington, 2012; Smerdon et al., 2003), Canada (Beltrami & Kellman, 2003; Zhang et al., 2005), and Europe (García-Suárez & Butler, 2006; Jungqvist et al., 2014) all report evidence of soil warming in the recent past. Additionally, Cuesta-Valero et al. (2016) brought attention to the question of how global Earth system models (ESMs) simulate soil heat storage and reported that models participating in the Climate Model Intercomparison Project 5 (CMIP5) projected considerable warming at 1-m depth and generally follow the warming trajectories as for surface air temperature. García-García et al. (2019)

Investigation: Jennifer L. Soong, Claire L. Phillips, Catherine Ledna, Charles D. Koven

Methodology: Claire L. Phillips, Charles D. Koven, Margaret S. Torn

Project administration: Jennifer L. Soong, Margaret S. Torn

Supervision: Jennifer L. Soong, Margaret S. Torn

Visualization: Jennifer L. Soong, Claire L. Phillips

Writing - original draft: Jennifer L. Soong, Claire L. Phillips

Writing - review & editing: Jennifer L. Soong, Catherine Ledna, Charles D. Koven, Margaret S. Torn

subsequently demonstrated that in CMIP5 simulations, the coupling of soil and air temperatures is strongly affected by the presence of snow cover and soil freezing phenomena in winter and by canopy cover and precipitation rates in summer.

Temperatures near the soil surface are influenced by multiple energy-exchange processes, including interactions between heat exchange and water evaporation, that could result in soils warming faster, slower, or at similar rates as the air temperatures above, depending on factors such as incident radiation, snow cover, soil ice, soil moisture, or land cover (Schmidt et al., 2001). In areas with freezing winter conditions or high soil moisture, effective thermal diffusivity may be reduced substantially by the insulating effects of snow cover and latent heat used in thaw and evaporation. In one of the only studies of climate change predictions for soils, in North America, climate change was predicted to warm soil and air temperatures by the same amount in the South while the ratio of air:soil warming was <1 in colder, Northern regions, indicating that soil warming is predicted to lag behind air warming (García-García et al., 2019).

Soil orders reflect the full suite of ecosystem state factors (Jenny, 1941), particularly climate, geomorphology, biota, and landscape age, and are good indicators of land uses. The degree to which carbon-rich soils in high-latitude permafrost (Gelisol) and boreal (Spodosol) regions warm in the future may have a stronger impact on the release of soil carbon to the atmosphere and its positive feedback to atmospheric warming than will warming of tropical (Ultisol and Oxisol) regions (Koven et al., 2011; Oechel et al., 1993). Soil order distributions can also be used to map warming effects on major natural resource land uses such as agricultural production (Mollisols) and forestry (Alfisols). Warmer atmospheric temperatures have been shown to reduce some crop yields and are predicted to negatively affect global yields of key staple crops grown mainly in Mollisol regions, such as wheat, maize, and barley (Hatfield et al., 2011; Lobell & Field, 2007; Zhao et al., 2017). Changes in agriculturally relevant temperature thresholds, such as a reduction in the number of days below freezing per year, will be particularly relevant in soil orders used heavily in food or timber production (Brown & Blackburn, 1987). Thus, soil orders can be useful for categorizing climate change impacts on regions defined by the distribution of certain soil types.

To understand the impacts of climate change on soils, it is necessary to characterize the change in soil throughout the soil profile, not just in the top few centimeters. Soil temperature is one of the primary determinants of soil microbial activity and soil organic matter decomposition rates, which largely determine nutrient availability and soil greenhouse gas fluxes (Davidson & Janssens, 2006; Koch & Kandeler, 2007; Lloyd & Taylor, 1994). Subsoils, below 20 cm, contain more than 50% of global soil organic carbon stocks (Jobbágy & Jackson, 2001; Schmidt et al., 2011). In a forest experiment, warming the whole soil profile by 4°C increased decomposition in the subsoil by 35% (Hicks Pries et al., 2017). If extrapolated globally, Hicks Pries et al. estimate that these results imply that subsoils below 30 cm could lose an additional $3.1 \text{ Pg C} \cdot \text{year}^{-1}$ with warming in comparison to surface-soil-warming-only estimates. The rate and extent to which the climate signal will propagate downward and warm deeper soil is a function of the effective soil thermal conductivity, which can vary widely, between $0.05\text{--}1 \text{ W} \cdot \text{m}^{-1} \cdot ^{\circ}\text{C}^{-1}$ for dry soil of different soil types due to variations in soil texture, moisture, porosity, and structure (Ochsner et al., 2000; Zhang & Wang, 2017). Understanding whether deep soil warming will occur at a similar rate as surface soils will greatly improve our ability to predict the magnitude of responses of temperature-sensitive soil processes such as decomposition, nutrient cycling, and the production of greenhouse gases.

This paper has three main objectives. The first objective is to quantify change in global soil temperatures and moisture predicted over the 21st century, spatially and by soil type. We examined soil temperature and moisture predictions to 2100 from 14 ESMs from CMIP5 by soil order, to relate spatial patterns in warming to the different roles of soils as a primary natural resource. The second objective is to test the hypothesis that soil warming down to 100-cm depth will keep pace with warming at the soil surface and with air warming above it. The third objective is to evaluate ESM performance in representing thermal properties from observed data. We compiled observations of air and soil temperatures from over 660 meteorological and eddy covariance stations globally and compared global patterns in air-ground coupling with modeled patterns of air-ground coupling. In addition to evaluating CMIP5 predictions at multiple depths, we also conducted a simple simulation of one-dimensional soil heat transport using Hydrus 1D (Šimůnek et al., 2013). This provided a simplified environment in which we could impose a large warming signal at the soil surface and explore the lags in warming at 100 cm that could be expected in soils of varying thermal conductivity.

2. Methods

2.1. Analysis of ESMs

We compared ESMs from 14 modeling groups in the CMIP5 ensemble (Table S1). ESM data were downloaded from the World Climate Research Program (<https://esgf-node.llnl.gov/search/cmip5/>). We excluded CMIP5 ESMs that did not report depth layer-specific soil temperatures. For models that did not report layer-specific soil moisture, we analyzed temperature only. We selected the first ensemble model version from each group denoted as r1i1p1, except for CCSM4 where we used r2i1p1, as these are the model versions used in other CMIP5 experiments (i.e., García-García et al., 2019). To compute model ensemble averages, we regressed the ESM air surface temperature (tas; usually at 2 m above 2/3 of the obstacle height; Taylor et al., 2012), soil temperature (tsl), and soil moisture (mrlsl) outputs to a common grid size (288 × 192 lon/lat, as used in CCSM4) using the ncremap tool in the netCDF operator language (Zender, 2008). In the case of higher-resolution models being regressed to a lower resolution, the lower-resolution grid cells with greater than 10% data coverage were area-weighted based on the source data, and grid cells with less than 10% coverage were classified as missing values. Grid cells that contained land and ocean were weighted by the percent land area occupying the grid cell for the calculation of air surface temperature over the land.

Soil geometry differs substantially among the models (Table S1), with the total number of layers ranging from 3 to 23 and the depth of the soil lower boundary ranging from 3 to 43 meters (Slater & Lawrence, 2013). To enable comparison across models, we assumed that the temperature at the midpoint of each layer was equal to the mean temperature for the whole layer and linearly interpolated to 1 and 100 cm when models did not already report soil temperature at those depths. We explored both linear and logarithmic interpolation and found that linear fits best represented observed trends. For models where the midpoint of shallowest soil layer is greater than 1-cm deep, we instead report the midpoint of the shallowest soil layer, which was 5 cm for CanESM2, GISS-E2R, and HadGEM2-ES; 1.8 cm for IPSL-CM5A-LR; 2.5 cm for MIROC5; and 3.0 cm for MPI-ESM-LR. For simplicity, we refer to this near-surface depth nominally as 1 cm here.

We report temperature and moisture data for the end of the 21st century (EOC) as a 20-year average value of years 2081–2100 and for the historic period as a 20-year average value of years 1986–2005. We report the temperature change over the 21st century as the difference between these two periods. We also used the standard error of the 14 ESM model predictions for the EOC to evaluate the relative degree of agreement between the ESMs around the ensemble mean predictions.

To compare predictions of air and soil warming trends by the CMIP5 model ensemble, we calculated the air-soil warming offset as the difference between air and soil warming (at 100-cm depth) predictions for the EOC. We made the same air-soil offset calculation for annual time steps to examine trends in the air-soil warming offset predictions over time, both globally and by soil order.

We analyzed ESM predictions for the RCP 4.5 and RCP 8.5 emission scenarios, which correspond to 4.5 and 8.5 W m⁻² forcing by 2100, representing intermediate and low levels of mitigation, respectively (Van Vuuren et al., 2011).

2.2. Estimation of Seasonal Fluctuations in Soil Temperature

We examined the change in seasonal soil temperature cycles at 1-cm depth between the historic and EOC periods for different soil order regions. We did this separately for the Northern and Southern Hemisphere grid cells and plotted the CMIP5 ensemble mean of the monthly output data. We were interested in the change in the number of days below freezing between the historical and EOC periods since freezing temperatures can influence the emergence of seeds and viability of crops (Boyd & Lemos, 2013). Thus, we used a linear interpolation between the monthly temperature predictions to estimate the approximate change in the number of days below freezing (0 °C) between the historical and EOC periods.

2.3. Soil Order Classification

We characterized changes in soil temperature and moisture by soil order based on the Global Soil Regions Map data (Figure S1), which groups soil orders by the U.S. classification scheme (FAO-UNESCO & USDA-NRCS, 2005). This is the same map used by most ESM's to classify texture in their soil temperature

simulations (Table S1). Most soil orders in the U.S. classification have similar equivalents in the FAO scheme (Table S2). The soil order data were regredded to the common grid used in all our analyses (288×192 lon/lat) using the ncremap tool in the netCDF operator language (Zender, 2008).

We calculated average soil temperature and moisture for each soil order by first calculating the land area in each grid cell. We then determined the percentage of each land grid cell that corresponded to each of the 14 soil orders (including rock and shifting sand). Finally, we used the fraction of each grid cell corresponding to a given soil order to calculate area-weighted average values of temperature and moisture for each soil order. We used this method to extract the soil temperature and moisture data for each soil order from each of the ESM model outputs.

We focused our analysis on seven soil orders that are predominantly distributed latitudinally and correspond to certain biomes. These are Gelisols (permafrost), Spodosols (boreal and heathland), Alfisols (forest), Mollisols (grassland), Aridisols (desert), Ultisols (tropics), and Oxisols (tropics), in approximately decreasing latitudinal order.

In addition to analysis of warming for 14 major soil orders globally, we examined individual ESM soil temperature profiles for three regions with contrasting soil climates to illustrate the range of soil thermal conductivity predictions for contrasting biomes in RCP 8.5 for the EOC. These regions were defined as permafrost soils represented by Gellisol-dominated grid cells in Canada (bounded by $52\text{--}90^\circ\text{N}$, $140\text{--}60^\circ\text{W}$), temperate grassland soils represented by Mollisol-dominated grid cells in the U.S. Great Plains (bounded by $35\text{--}55^\circ\text{N}$ and $90\text{--}115^\circ\text{W}$), and tropical soils represented by Oxisol-dominated grid cells in the Amazon Basin (bounded by $5^\circ\text{N}\text{--}18^\circ\text{S}$, $80\text{--}40^\circ\text{W}$).

2.4. 1-D Simulation of the Range in Heat Transfer Down the Soil Profile

In an ESM model simulation, the soil temperature profile is affected not only by soil physics, but also by the projected rainfall and air temperature cycles. To isolate the effects of temperature alone, we examined the response time of the whole profile to surface warming in a simplified system, using a one-dimensional model that has the same basic conductive-diffusive heat transfer components as the ESMs. We used the Hydrus-1D model of soil heat transport to simulate how quickly heat is transferred from the soil surface to deeper soils in response to a 5°C step increase in surface temperature (Šimůnek et al., 2013). This simulation also provides a shorter time resolution than the CMIP5 20-year averaging, which can be used to examine rates of predicted thermal diffusion down the soil profile.

A 10 m deep soil profile was discretized into 200 layers, with layer thickness gradually increasing from 2.5 cm at the surface to 7.5 cm at the bottom. While the CMIP5 ESMs vary greatly in their soil depth and discretization (Table S1), we chose a 10-m lower boundary condition due to its minimal influence on soil heat transport to 1-m depth (Shufen & Xia, 2004; Smerdon & Stieglitz, 2006). Soil properties were homogenous throughout the profile with no snow layers. We conducted two simulations representing thermal properties for a clay and a sandy soil with water contents at field capacity in order to estimate the range of thermal diffusivity between two contrasting soil types. Soil porosity was prescribed as 50% for the clay and 40% for the sandy soil. Volumetric water content at field capacity was estimated as 39% and 7.4%, respectively, using the model's default hydraulic parameters for clay and sand.

The Hydrus-1D model implements one-dimensional heat transfer with the following convection-dispersion equation (Šimůnek et al., 2013)

$$C_p(\theta) \frac{\partial T}{\partial t} = \frac{\partial}{\partial x} \left[\lambda(\theta) \frac{\partial T}{\partial x} \right] - C_w q \frac{\partial T}{\partial x},$$

where T is temperature, x is depth, t is time, q is Darcian fluid flux density (units of length per time), θ is volumetric water content, $\lambda(\theta)$ is apparent soil thermal conductivity, and $C_p(\theta)$ and C_w are the volumetric heat capacities of the porous medium and the liquid phases, respectively. The first term on the right side represents heat flow by conduction, and the second term represents heat transported with water, where q is the water flux. Thermal conductivity was estimated as a function of soil water content as described by Chung and Horton (1987):

$$\lambda(\theta) = b_1 + b_2\theta + b_3\theta^{0.5},$$

where b_1 , b_2 , and b_3 are empirical coefficients established as -0.197 , -0.962 , and 2.521 for clay soil and 0.228 , -2.406 , and 4.909 for sandy soil. (Note that as originally parameterized, residual water content in the clay soil was equal to $0.03 \text{ cm}^3 \text{ cm}^{-3}$, and therefore, λ did not assume negative values.) Volumetric heat capacity was calculated following DeVries (1963), where $C_p(\theta)$ equals the sum of the heat capacities for the solid and water phases of the soil, with each component weighted by its volumetric fraction.

Simulations were run at a time step of 0.1 days for a 10-year period. The surface and the soil profile were initialized to 15°C . After initialization with a constant temperature, surface temperature was increased from 15 to 20°C in a step change on Day 30. Soil water content remained constant. A prescribed surface temperature provided the upper boundary condition for the soil domain, and a zero-temperature gradient was used as the lower boundary condition.

2.5. Analysis of Observational Data

In order to evaluate ESM performance in representing observed soil thermal properties, we obtained average soil and air temperature observations from meteorological and eddy covariance networks, for a total of 660 locations spanning various time periods (Figure 7; Table S3). In the United States and Europe, where a large number of records were available, we used only sites that had 10 or more years of data. In other regions, we used sites reporting at least one complete year of data (Table S3). All of the stations that were established for the purpose of weather monitoring are located in the open without tree cover, including the U.S. Climate Reference Network (USCRN) and Historic Russian Soil Temperature (HRST) stations, and the majority of the Soil Climate Analysis Network (SCAN) sites. These sites have land cover of forest, natural or cultivated grass, or bare soil and were characterized as grassland, forest, permafrost, or other categories. Eddy covariance sites had less managed vegetation and accounted for all of our forest observations along with six SCAN stations located in forests.

We calculated two variables for the observational data that characterize soil thermal properties. First, we calculated the mean offset between air and soil surface temperature (ΔT_{surf}), and between surface soil and deep soil temperatures (ΔT_{deep}):

$$\bar{T}_{\text{surf}} = \bar{T}_S - \bar{T}_{\text{air}}, \quad (1)$$

$$\bar{T}_{\text{deep}} = \bar{T}_D - \bar{T}_S, \quad (2)$$

where T_{air} is the mean temperature of the air, T_S is the mean temperature in the shallow soil, and T_D is the mean temperature in soils at 100 cm. Surface soil temperature observations were typically measured between 2 – 8 cm (5-cm placement was most common). The placement depth of deep soil measurements was more variable among sites. Therefore, to estimate temperature at 100 cm, we performed a linear regression using all the depths if data were available for at least three depths between 50 and 150 cm. Weather stations reported daily temperature, and flux stations reported half-hourly temperatures, which we averaged to monthly values for consistency with CMIP5 output. We omitted years where $>10\%$ of the data were missing. Temperature time series were plotted and visually inspected to determine that the remaining missing data did not impose a seasonal bias. We also plotted ESM modeled ΔT_{surf} and ΔT_{deep} using 1 cm as T_S for the historical period for Mollisol (grassland), Alfisol (forest), Gelisol (permafrost), and all other global grid cells to compare the shapes of the ΔT_{surf} and ΔT_{deep} temperature response curves from the models to the observational data, as in Koven and Stern (2013). We compared modeled and observed patterns in ΔT_{surf} and ΔT_{deep} in order to evaluate model variance in their ability to recreate observed patterns between ΔT_{surf} , ΔT_{deep} and mean annual temperature at a global scale.

3. Results

3.1. Predicted Soil Warming Over the 21st Century for RCP 4.5 and RCP 8.5

Globally, the 14-model CMIP5 ensemble mean predicted that soil temperatures at 1 cm increase by $4.5 \pm 1.1^\circ\text{C}$ (mean \pm SD) by the EOC under the high emissions RCP 8.5 scenario and by $2.3 \pm 0.7^\circ\text{C}$ under the lower emissions RCP 4.5 scenario (Table 1). Soil temperatures at 100 cm were predicted to increase by the nearly

Table 1

Global and Soil Order-Specific Mean \pm Standard Deviation of 14 CMIP5 Model Predictions for the Change in Near Surface Air, 1-cm Soil, and 100-cm Soil Temperatures Between the Historic Period (1986–2005) and the End of Century Period (2081–2100) for RCP 8.5 and RCP 4.5

	RCP 8.5 temperature change ($^{\circ}$ C)			RCP 4.5 temperature change ($^{\circ}$ C)		
	Air	1-cm soil	100-cm soil	Air	1-cm soil	100-cm soil
Global	4.85 \pm 0.93	4.50 \pm 1.13	4.45 \pm 1.10	2.46 \pm 0.63	2.26 \pm 0.68	2.26 \pm 0.66
Alfisol	4.45 \pm 0.85	4.17 \pm 1.05	4.13 \pm 1.04	2.27 \pm 0.58	2.05 \pm 0.62	2.04 \pm 0.59
Andisol	4.10 \pm 0.78	3.70 \pm 0.90	3.63 \pm 0.86	2.10 \pm 0.53	1.81 \pm 0.56	1.79 \pm 0.53
Aridisol	4.54 \pm 0.82	4.51 \pm 0.93	4.48 \pm 0.94	2.29 \pm 0.59	2.25 \pm 0.60	2.25 \pm 0.59
Entisol	4.47 \pm 0.82	4.47 \pm 0.91	4.43 \pm 0.92	2.24 \pm 0.61	2.21 \pm 0.64	2.21 \pm 0.63
Gelisol	7.14 \pm 1.65	5.93 \pm 2.06	5.82 \pm 1.93	3.66 \pm 1.00	3.17 \pm 1.07	3.18 \pm 1.05
Histosol	5.33 \pm 1.16	4.34 \pm 1.54	4.33 \pm 1.41	2.77 \pm 0.76	2.21 \pm 0.89	2.24 \pm 0.81
Inceptisol	5.01 \pm 1.00	4.35 \pm 1.30	4.31 \pm 1.23	2.54 \pm 0.65	2.19 \pm 0.74	2.20 \pm 0.70
Mollisol	4.94 \pm 0.95	4.44 \pm 1.19	4.38 \pm 1.16	2.53 \pm 0.66	2.21 \pm 0.67	2.21 \pm 0.64
Oxisol	4.22 \pm 1.06	4.18 \pm 1.13	4.14 \pm 1.15	2.11 \pm 0.66	2.06 \pm 0.67	2.06 \pm 0.67
Spodosol	5.64 \pm 1.23	4.36 \pm 1.69	4.29 \pm 1.53	3.01 \pm 0.79	2.27 \pm 0.97	2.23 \pm 0.82
Ultisol	3.95 \pm 0.83	3.90 \pm 0.91	3.87 \pm 0.90	2.01 \pm 0.55	1.94 \pm 0.58	1.94 \pm 0.57
Vertisol	4.03 \pm 0.82	4.01 \pm 0.98	3.97 \pm 0.99	2.03 \pm 0.55	1.98 \pm 0.61	1.98 \pm 0.60

the same amount per year as at 1-cm depth resulting in warming of 4.5 ± 1.1 and 2.3 ± 0.7 $^{\circ}$ C for the EOC under RCP 8.5 and RCP4.5 respectively (Figures 1a and 1e). In comparison, global air temperatures were predicted to warm by 4.8 ± 0.9 and 2.5 ± 0.6 $^{\circ}$ C over the same period for RCPs 8.5 and 4.5, respectively (Figures 1b and 1f). We found no difference in the warming predictions for near-surface (1 cm) versus deep (100 cm) soil layers globally or for any of the soil orders (Table 1; Figures 2 and S2).

Soil warming generally followed the same spatial pattern as that of air warming, with the greatest warming occurring at higher latitudes (Figure 1). Permafrost (Gelisol) regions were predicted to have the highest soil warming while soil orders in tropical (Ultisol and Oxisol) regions showed the lowest soil warming (Figures 2 and S2). Based on the standard error of CMIP5 model warming predictions for the EOC, model agreement on predicted soil warming was lowest for Gelisols, Histosols, and Spodosols and highest for Andisols, Entisols, and Ultisols (Table 1).

All of the CMIP5 ensemble members predicted rapid propagation of the warming signal from the soil surface downwards; however, they varied in the degree of warming predicted by the EOC (Figure 3). In our test regions of Canadian Gelisols, U.S. Mollisols, and Amazonian Oxisols, all ensemble members predicted homogeneous warming (i.e., <0.5 $^{\circ}$ C difference) throughout the soil profile layers, some down to over 10-m depth (Figure 3). MIROC5 had a modest vertical gradient in warming in Canadian Gelisol regions, with near-surface layers predicted to warm about 0.5 $^{\circ}$ C more than deep soil or than air by end of century. HadGEM2-ES also predicted a decrease in warming intensity within the first meter of the soil. In contrast, GFDL-ESM 2G predicted increased warming over the first one meter of the soil in U.S. Mollisols.

The ratio of soil to air warming would be one if soil and air temperatures change by the same amount by the EOC. The models predicted a soil-to-air warming ratio of one in the Amazon Oxisol region, but mostly predict a ratio of less than one in U.S. Mollisols and Canadian Gelisols regions (Figure 3d, e & f). The spread in model predictions of the soil-to-air warming ratio was greatest in the Canadian Gelisol region, with one model, MIROC5, even predicting greater soil warming compared to air warming (i.e., soil-to-air warming ratio > 1 ; Figure 3d).

3.2. Soil Warming in Comparison to Air Warming Over the 21st Century

The CMIP5 ensemble mean prediction of the global air-soil warming offset, estimated as the change in air temperature between the historical and EOC periods minus the change in soil temperature (at 100 cm) over the same period, was 0.20 ± 0.91 (mean \pm SD) for RCP 4.5 and 0.40 ± 1.4 for RCP 8.5 (Figures 1c and 1g). This means that globally, this CMIP5 ensemble predicted slightly more warming of air than the soil below. This greater-than-zero air-soil warming offset was predicted by all of the ESMs except IPSL-CM5A-LR, which, unlike any of the other ESMs, predicted an air-soil warming offset of less than zero for all soil orders and for the global land area for RCP 8.5 and 4.5 (Table S4).

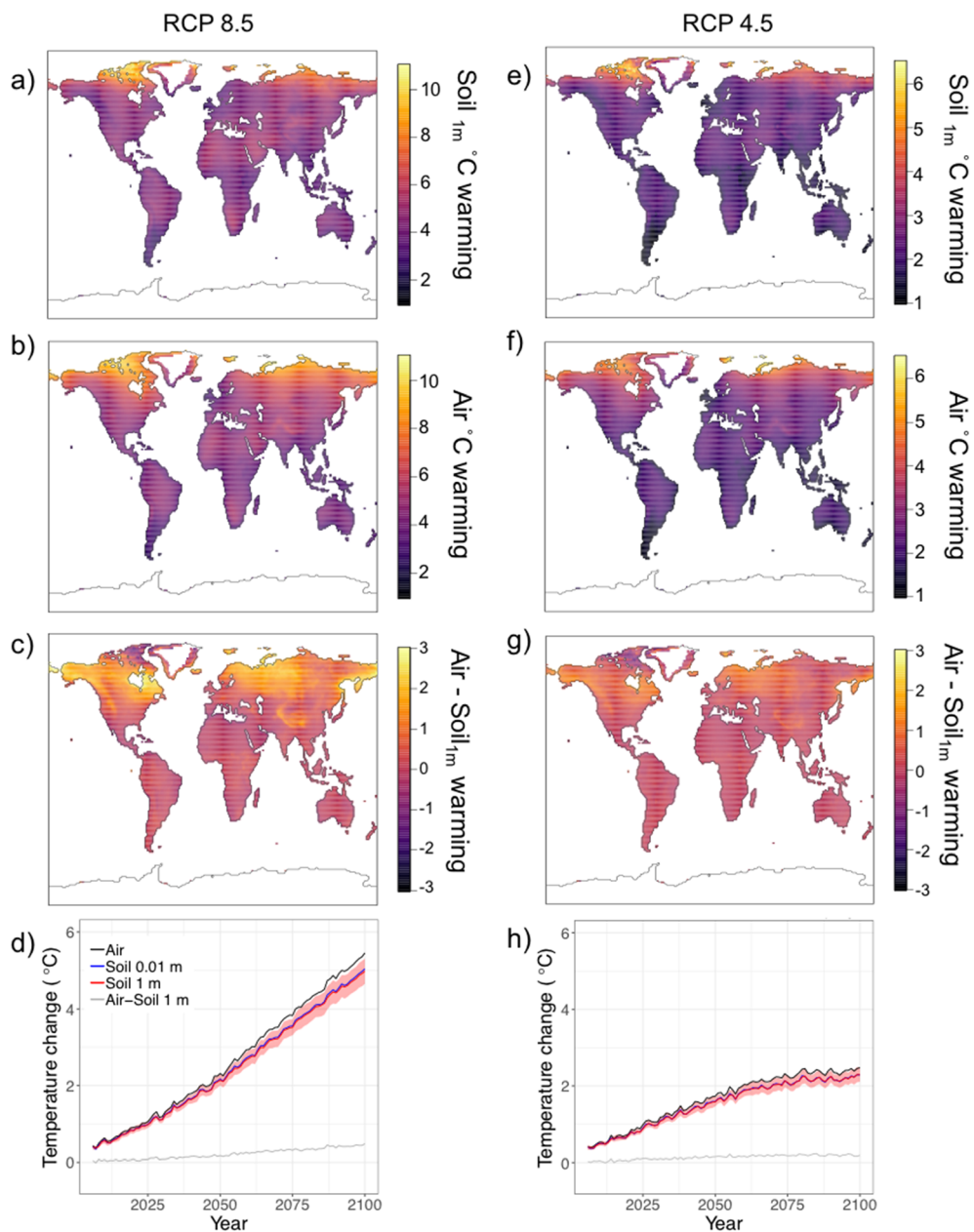


Figure 1. Climate Model Intercomparison Project 5 (CMIP5) ensemble mean predictions of warming between the historical period (1986–2005) to the end of century period (2081–2100) for RCP 8.5 (a–d) and RCP 4.5 (e–h). (a,e) Soil warming prediction at 1-m depth. (b,f) Near-surface air warming prediction. (c,g) difference between warming in the air and in the soil at 1-m depth. (d,h) annual time series output of CMIP5 ensemble mean predictions for the global change in air and soil temperature over the 21st century as compared to the historical period. One standard error of the 14 model predictions is shown by the pink ribbon around the ensemble mean predictions of warming, in red, at 1-m depth.

When analyzed by soil order, biome-specific variations in ensemble mean air-soil warming offsets emerged. In higher-latitude biomes, mean air warming trends fell outside of the standard error of the mean soil warming predictions at 1 m, while in desert and tropical regions, they were indistinguishable (Figure 2). The most extreme cases were in Gelisols, Histosols, and Spodosols, which are present at high latitudes and had an average predicted air-soil warming offset of 1.3, 1.0, and 1.4 °C, respectively, under RCP 8.5, and 0.49, 0.54 and 0.78, respectively, under RCP 4.5 (Table 1). Ensemble mean predictions for Alfisol and Mollisol regions also showed slightly lower soil warming compared to the above air warming by the EOC

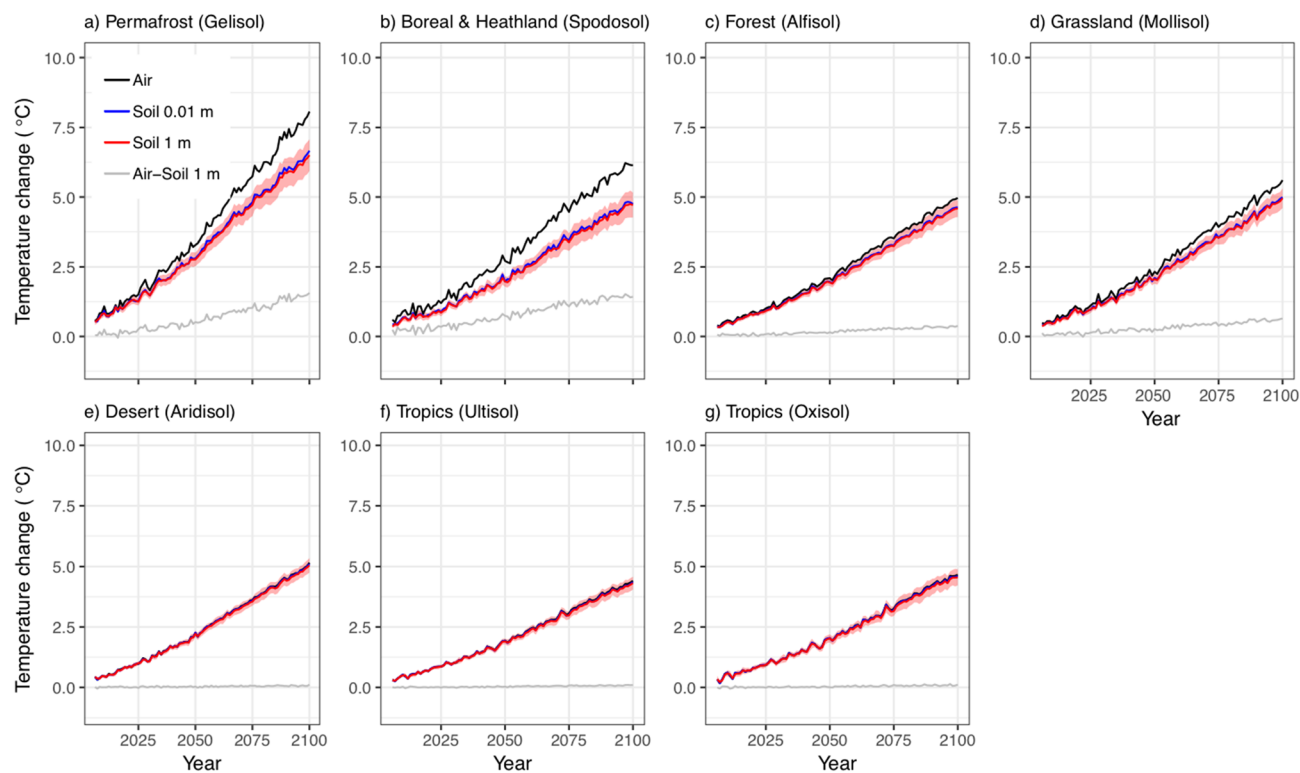


Figure 2. Time series of Climate Model Intercomparison Project 5 ensemble mean air and soil temperature change relative to the historical period (1986–2005) for RCP 8.5 for different soil orders, as well as the air-soil temperature difference. Panels show data covering different soil orders, which map closely to the indicated biome. The standard error of the 14 model predictions for soil temperature at 1-m depth is shown in the pink ribbon.

(Figure 2). This difference between soil and air temperature change increased over the 21st century. In summary, air warming slightly overestimated soil warming at a global scale, particularly in colder areas with high precipitation, but it accurately predicted soil warming in warm and dry regions. Thus, soil temperature predictions themselves provide a more accurate forecasting of changes in soil properties with climate change, particularly in cold-climate soils.

The CMIP5 prediction that deep soil warming would nearly keep pace with shallow warming was consistent with basic physical assumptions about soil thermal conductivity in the absence of interacting factors. This rapid heat transfer down the soil profile was confirmed by our HYDRUS-1D simulations, which showed the rates of transfer of warming from the surface to deeper soil depths in response to a step-wise increase in ground surface temperature from 15 to 20 °C (Figure 4). For a sandy soil with a relatively high rate of soil heat transport ($\lambda = 1.4 \text{ W}\cdot\text{m}^{-1}\cdot\text{K}^{-1}$, $C = 1.5 \text{ MJ}\cdot\text{m}^{-3}\cdot\text{K}^{-1}$), the simulation predicted that it would take 0.9 or 2.3 years for 90% of the temperature change to occur at 1- or 3-m depth, respectively. For a clay soil with a slower rate of heat transport ($\lambda = 1.0 \text{ W}\cdot\text{m}^{-1}\cdot\text{K}^{-1}$, $C = 2.6 \text{ MJ}\cdot\text{m}^{-3}\cdot\text{K}^{-1}$), it was predicted to take 1.7 or 4.6 years for 90% of the change to occur at 1- or 3-m depth, respectively. Thus, under the conditions of this simulation, the expected time lag between warming the ground surface and 1-m deep soils was less than 2 years.

3.3. Shifts in Seasonal Soil Temperature Trends by the EOC

The seasonal distribution of 1-cm soil warming predicted by CMIP5 models between the historical and EOC periods varied by soil order. In Northern Hemisphere soils in colder and temperate regions, such as Gelisols, Spodosols, and Mollisols, more warming was predicted in summer and winter than in spring and autumn (Figure 5). In comparison, Alfisols (temperate forest soils), Ultisols (tropical soils), and Oxisols (tropical soils) had a more even distribution of predicted warming throughout the year. For example, the magnitude of warming at 1 cm varied throughout the year in the Northern Hemisphere by 0.60 °C for Gelisols, 0.70 °C for Spodosols, and 0.59 °C for Mollisols, but only 0.31 °C for Alfisols, 0.09 °C for Ultisols, and 0.11 °C for Oxisols (Figure 5).

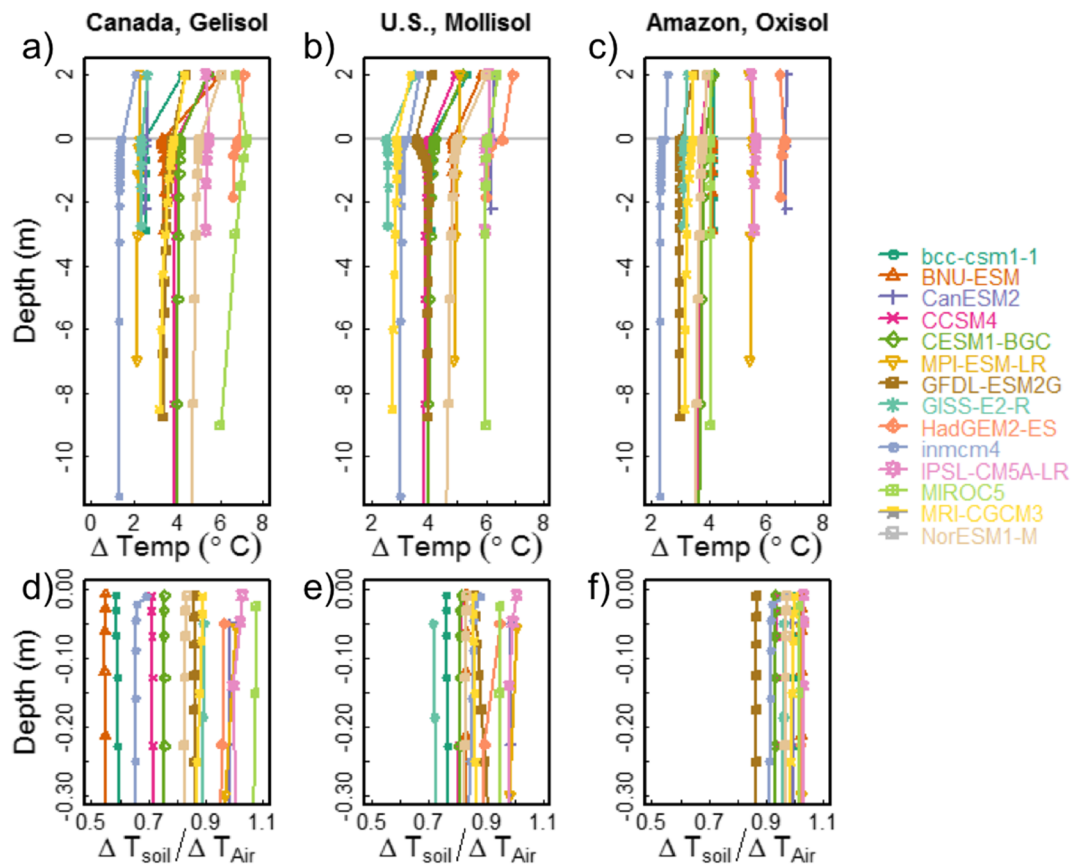


Figure 3. Individual earth system model, regionally averaged profiles of air and soil temperature change, RCP 8.5 for the end of century period (2081–2100) as compared to the historical period (1986–2005), for (a,d) Canadian Gelisols, (b,e) U.S. Mollisols, and (c,f) Amazon Oxisols. Depths shown are the model layer midpoints, and positive values refer to the height of air temperatures aboveground while negative values refer to soil temperature depths belowground. Panels d, e, and f show the ratio of soil-to-air temperature change for the given soil layers within each model.

Based on linear interpolation between ensemble mean predictions of monthly soil temperatures, the number of days above freezing (0°C) was predicted to decrease or sometimes disappear between the historical and EOC periods for different soil order regions. In Northern Hemisphere Mollisol regions, $<0^{\circ}\text{C}$ temperatures present in the historical period disappeared completely in the EOC. This equates to approximately 96 days for Northern Hemisphere Mollisols that were historically below freezing but will not experience $<0^{\circ}\text{C}$ temperatures in the EOC. Northern Hemisphere Gelisol regions experienced $<0^{\circ}\text{C}$ days in both the historical and EOC periods, but the number of days $<0^{\circ}\text{C}$ is predicted to decrease by approximately 44. Similarly, Northern Hemisphere Spodosol regions were predicted to have 56 fewer days $<0^{\circ}\text{C}$ in the EOC as compared to the historical period. In this analysis, Southern Hemisphere Gelisol, Spodosol, and Mollisols regions never reach 0°C or below based on where they are located in the soil order mapping (Figure S1). The locations of some soil orders, such as Gelisols, Spodosols, Alfisols, and Mollisols, are in much warmer regions in the Southern Hemisphere than the Northern Hemisphere, according to the Global Soil Regions map (FAO-UNESCO & USDA-NRCS, 2005). Similarly, global average soil temperatures for Alfisol, Aridisol, Oxisol, and Ultisol soil orders were never $<0^{\circ}\text{C}$ in either the historical or EOC period (Figure 5).

3.4. Predictions of Soil Moisture Change Over the 21st Century

In Gelisols, Spodosol, Alfisol, Ultisol, and Oxisol regions, the models predicted a general drying trend in soil moisture at 10-cm depth over the 21st century (Figure 6). More arid regions characterized by Mollisol and Aridisol soils showed strong model agreement; however, the drying trend was less pronounced than in wetter regions (Figures 6d and 6e). Based on the standard error between the ESM predictions, there was much

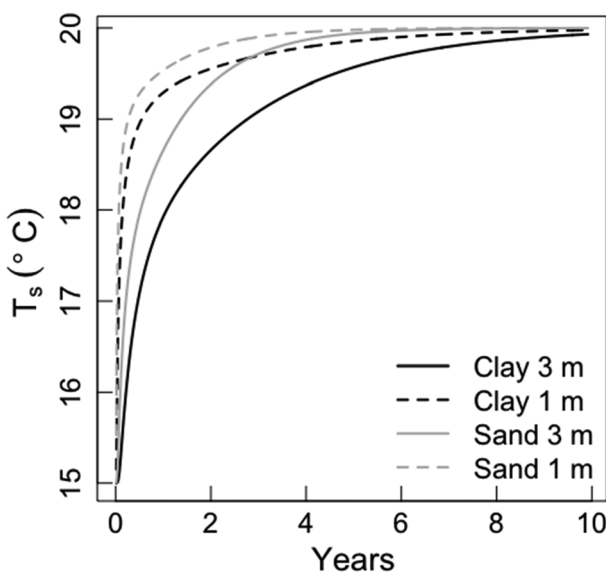


Figure 4. Simulation of the impacts of a 5 °C step increase in ground surface temperature on soil temperature at 1- and 3-m soil depths for thermal properties representing sand and clay texture soils.

the ΔT_{surf} observational patterns, three had simulated snow as the uppermost soil layer rather than a distinct snow layer (HadGEM-ES, IPSL-CM5A_LR and MPI-ESM-LR). The other three models, including

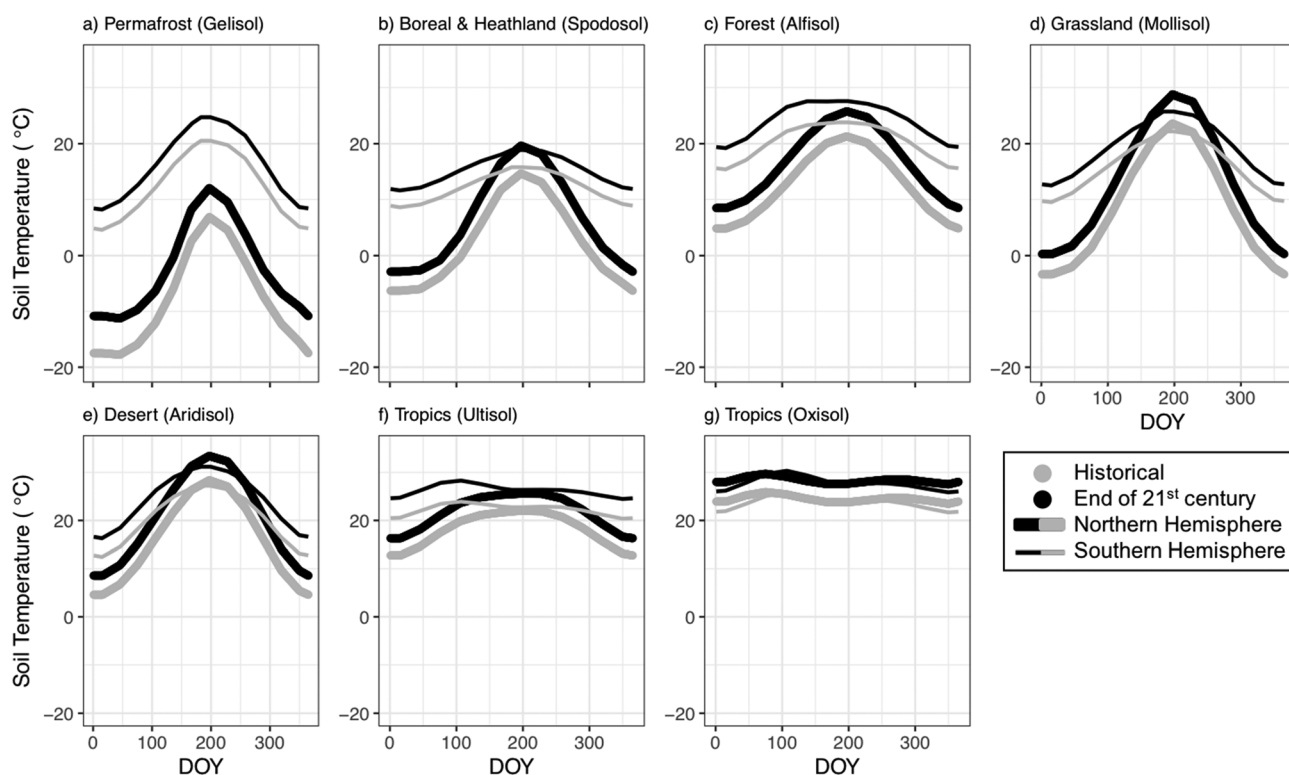


Figure 5. Ensemble mean soil temperature at 1 cm for the historical period (1986–2005) in gray and end of century period (2081–2100) for RCP 8.5 in black across days of the year (DOY). Panels show data covering different soil orders, which map closely to the indicated biome. Thick lines are for the Northern Hemisphere, and thin lines are for the Southern Hemisphere. The southern hemisphere x axis has been adjusted to show Northern Hemisphere seasonal equivalence by adjusting DOY by 183 days.

lower model agreement in soil moisture change in the EOC for Gelisol and Spodosol regions than for lower-latitude regions (Figure 6).

3.5. Comparison of Observed and Modeled Soil Thermal Properties

Observations of the offset between air and shallow soil temperatures (ΔT_{surf}) showed distinct biome-specific trends in the global data set (Figure 7a), revealing a regionally biased offset between air and soil temperatures. In permafrost regions where snow regularly occurs, the observed ΔT_{surf} decreased linearly with air temperatures (Figure 7a). In snow-free regions, ΔT_{surf} was invariant with mean annual air temperature, but depends on vegetation cover. Forests tended to have lower ΔT_{surf} than did grasslands with the same mean annual air temperature.

Most of the CMIP5 models were able to recreate the same temperature response patterns in ΔT_{surf} and ΔT_{deep} as the observations from the historical period (Figures 8a and 8b). Eight of the fourteen models replicated the temperature patterns observed at permafrost sites of decreasing ΔT_{surf} at progressively warmer temperatures below 0 °C (bcc-csm1-1, BNU-ESM, CCSM4, CESM1-BGC, GISS-E2-R, inmcm4, MRI-CGCM3, NorESM1-M; Figure 8a). These eight models also showed an increase in ΔT_{surf} between -20 and -12 °C mean annual temperature. Our observational data set had few points less than -12 °C mean annual temperature, but could support these model predictions. Of the six models that failed to replicate

these model predictions, three had simulated snow as the uppermost soil layer rather than a distinct

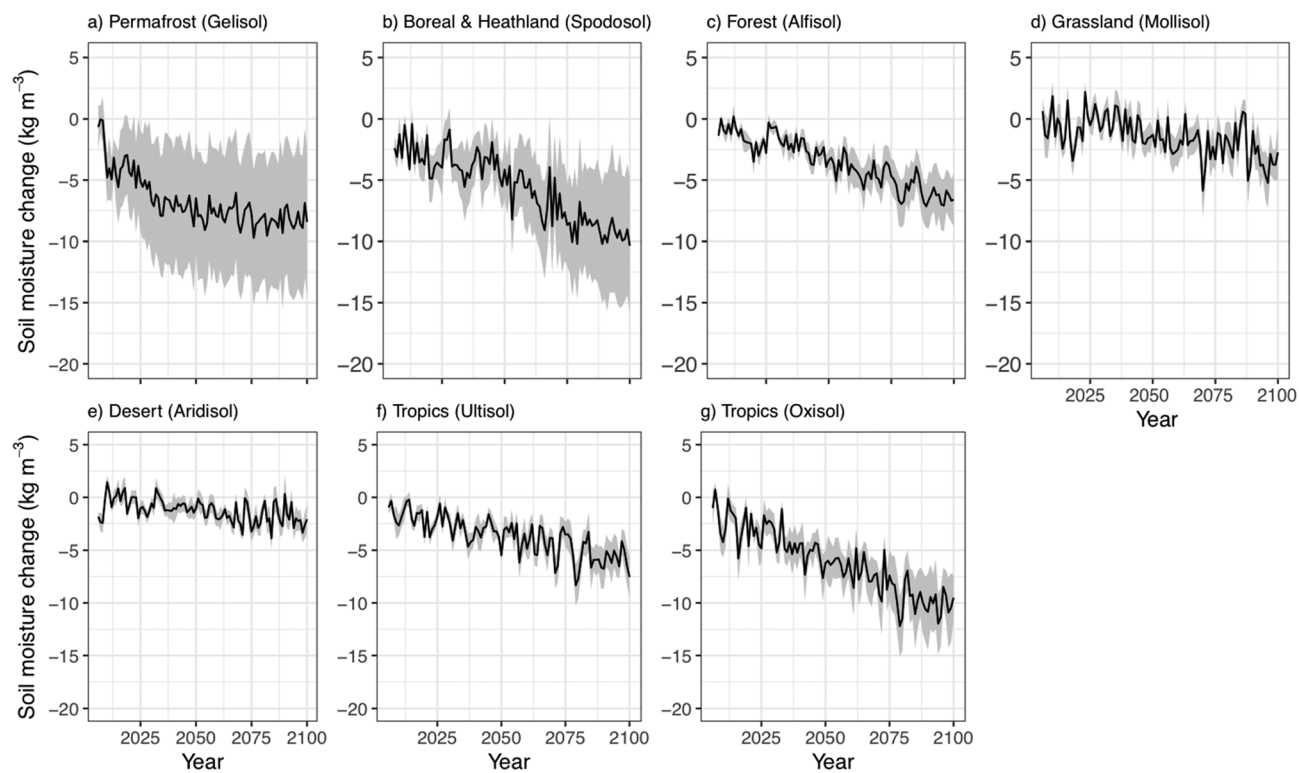


Figure 6. Climate Model Intercomparison Project 5 ensemble mean predictions for the change in soil moisture as compared to the average soil moisture during the historical period (1986–2005) at 10-cm depth for RCP 8.5 (black line). Panels show data covering different soil orders, which map closely to the indicated biome. Grey ribbon shows one standard error calculated from the 14 model predictions for annual estimates.

GFDL-ESM 2G, CanESM2, and MIROC5, also had a very weak increases in ΔT_{surf} relative to observations (Figure 8a).

We found no offset between mean annual temperature at the soil surface and 1-m depths for observations ($\Delta T_{\text{deep}} \approx 0$), regardless of climate or vegetation type (Figure 7b). Six ESMs predicted $\Delta T_{\text{deep}} < 0$ in permafrost regions (Figure 8b). Some, but not all, of these models included thermal representations of organic soils (Table S1), including a lower thermal conductivity and higher heat capacity relative to mineral soils (Lawrence et al., 2011). All of the CMIP5 ensemble members using the CLM3 and CLM4 land models predicted $T_{\text{deep}} < 0$ in permafrost regions (including CCSM4, CESM-BGC, and Nor-ESM 1), while two other models that used derivatives of CLM predicted $T_{\text{deep}} \approx 0$ (BNU-ESM and BCC-CEM1-1). All of the ensemble members that predicted $\Delta T_{\text{deep}} > 0$ in permafrost regions were those that represented snow as upper soil layers rather than as a distinct snow layer above the soil surface.

4. Discussion

4.1. Predicted Soil Warming Over the 21st Century

Soil temperatures will rise steadily over the 21st Century, though at a slightly slower rate than air temperatures, resulting in global average warming in the top 1 m of soil of 4.5 and 2.3 °C for the CMIP5 RCP 8.5 and 4.5 scenarios, respectively (Figure 1). The global pattern of soil warming generally follows the spatial pattern of atmospheric warming, with greater warming at high latitudes and less in the tropics. Air temperatures in high latitudes are predicted to increase significantly faster than those in lower latitudes owing to thawing ice-albedo and water-vapor feedbacks, frequently referred to as polar amplification of warming (Bekryaev et al., 2010; Holland & Bitz, 2003). However, the presence of ice and snow cover reduces the rate of soil warming and leads to a greater offset between air and soil temperatures at high latitudes over the century (Smerdon et al., 2004; Zhang, 2005; Zhang et al., 2001). These results are in agreement with snow insulating effects and latitudinal trends in the air-soil warming offset found across North America

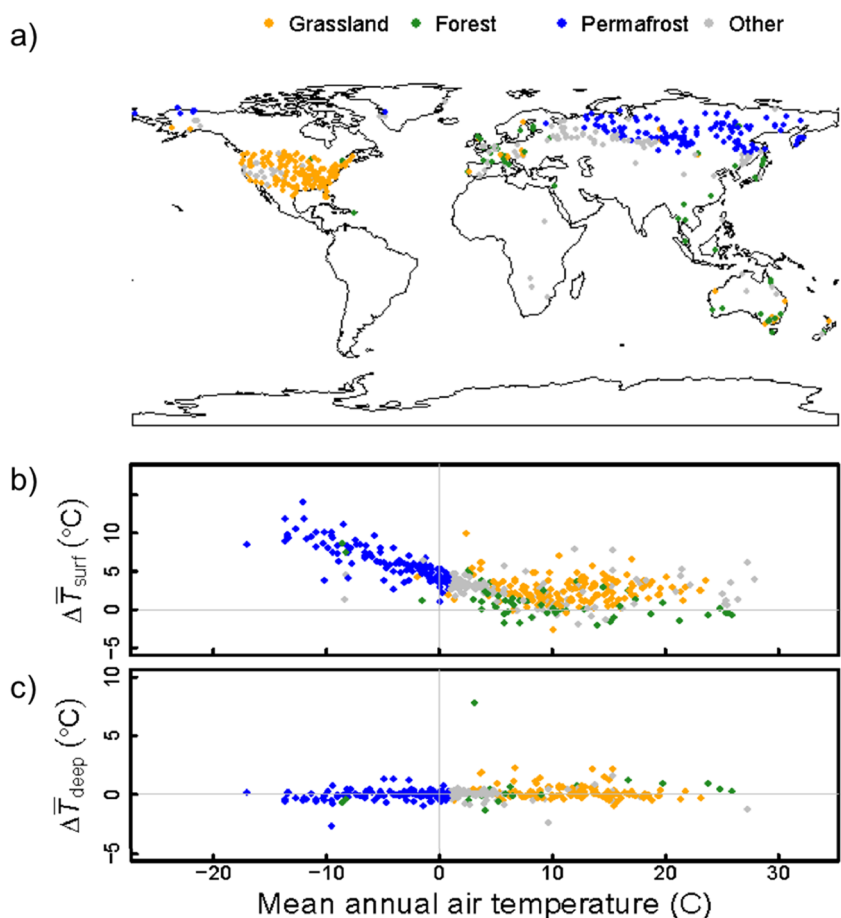


Figure 7. Observational data (a) location of the observation stations, (b) difference between shallow-soil and surface-air temperature (T_{surf}), and (c) difference between shallow-soil and deep-soil temperature (T_{deep}) for grassland, forest, permafrost, and “other” regions.

(García-García et al., 2019). Snow cover insulates the soil near the freezing point, even when air temperatures are much colder (Maurer & Bowling, 2014; Sokratov & Barry, 2002; Zhang, 2005). Despite this effect, high-latitude soils are still projected to warm faster than elsewhere, although at a slower rate than the surface air above them. The regional differences in future soil warming are important because warming will have different, regionally specific impacts on carbon-climate feedbacks and agricultural production, as discussed below.

Both shallow and 1 m deep soil temperatures are expected to warm at similar rates with an estimated time lag of less than 2 years between shallow and deep soil warming (Figure 4). This time lag is too short to be detected in predictions of 20-year averaged climate conditions. Several lines of evidence support the prediction of a short lag between shallow and deep soil warming. First, it is expected based on simple physical models of conductive heat transport in soil (Figure 4; Lesperance et al., 2010; Smerdon et al., 2003). Second, although there is a range in ESM predictions for the amount of warming expected by the EOC, predicted heat-transport and soil-to-air warming ratios are similar through all soil depths in the ESMs (Figure 3). This was true even for models that represent soil thermal conductivity as dependent on different soil properties such as organic carbon content. Finally, similar rates of shallow and deep soil warming are predicted for all soil orders over time (Figures 2 and S2).

4.2. Soil Warming in Relation to Air Warming

Comparison of predicted air and soil temperatures can be used to analyze differences in ESM model structures (García-García et al., 2019), as well as to validate the use of surface air warming as a proxy for soil warming over the 21st century. We used the difference between air-soil warming as a test of whether they

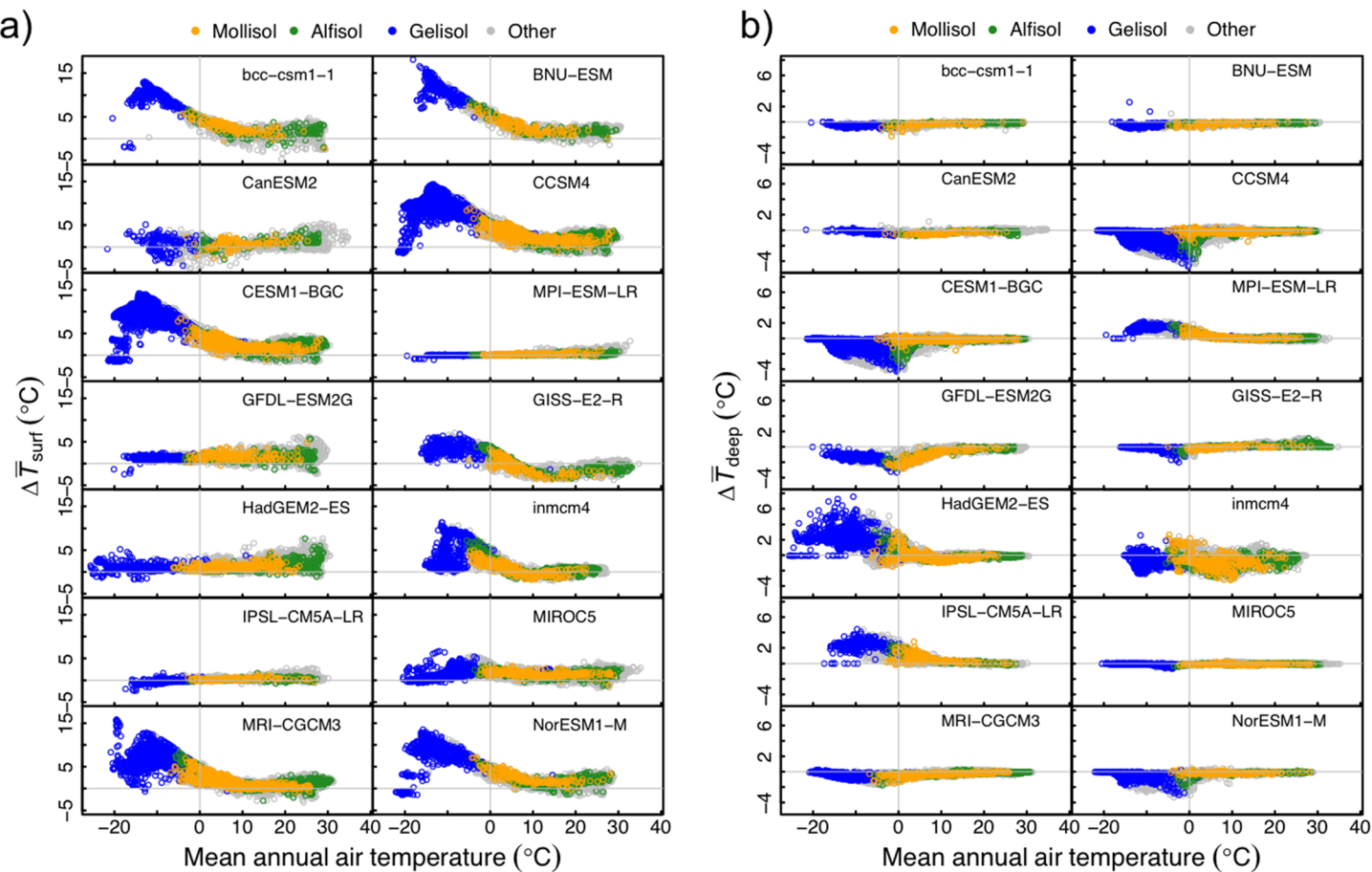


Figure 8. Individual Earth system model outputs of (a) difference between shallow-soil and surface-air temperature (T_{surf}) and (b) difference between shallow-soil and deep-soil temperature (T_{deep}) for Mollisol, Alfisol, Gelsol, and “other” soil types.

warm at the same rate. The global ensemble mean prediction for the air-soil warming offset was just over zero globally because snow and soil ice impede the transfer of the warming signal from air to the soil in some areas. Additionally, energy from the warmer air may be used for thawing frozen soil water rather than raising soil temperatures. Thus, the rate of surface air warming is a good proxy for expected soil warming in warm and arid regions, but not in cold and wet regions where surface air warming will outpace soil warming.

Although we found a rapid transfer of a 5 °C near-surface temperature step change to 1 m deep soils in less than 2 years in our HYDRUS-1D simulation (Figure 4), freezing phenomena, and energy and water fluxes at the surface can impede the direct transfer of the atmospheric temperature signal to the soil (Decker et al., 2003). This becomes apparent in the contrast between air and soil warming trends over the 21st century for soil orders characteristic of cold regions, such as Gelsols and Spodosols, as compared to soils from warmer and drier regions, such as Aridisols, Oxisols, and Ultisols (Figure 2). In contrast to the regional differences in air-to-soil warming trends, however, there was no difference between shallow (1 cm) and deep (100 cm) soil warming within any of the soil orders or globally.

A key question here was the extent to which polar amplification of atmospheric warming is also expressed in soil warming. At high latitudes, the loss of insulating snow cover with warming, and consequent increased wintertime transfer of heat from soils to the atmosphere and therefore cooling, might be expected to slow warming of soils in the region and offset the arctic amplification of surface air warming. The CMIP5 ESMs suggest, however, that this effect is minor compared to the overall atmospheric warming patterns, and high-latitude soils are still expected to warm more rapidly than those in the rest of the globe. Thus, polar amplification also applies, albeit more weakly, to soils.

The ESM ensemble predicts that the offset between air and soil warming is lower in the polar deserts and regions with less than -12°C mean annual temperature (Figure 8), than in the tundra and boreal regions (Figures 1c and 1g). At the highest latitudes, the polar deserts currently experience lower snowfall and less consistent snow cover than the boreal and tundra regions and thus have less of the insulating effects of snow cover. With warming, these polar desert regions are expected to receive more snow due to increased atmospheric moisture transport, and this increase of snow with warming leads to a further warming of the soils (Krasting et al., 2013). Thus, the boreal and wetter tundra regions, as well as the Himalayas, are the only regions of the planet where soils are expected to warm at an appreciably slower rate than surface air temperatures.

4.3. Model Comparison and Evaluation

The 14 CMIP5 ESM predictions for soil warming by the EOC showed less agreement than for air warming (Table 1). This is likely due to differences in the physical representation of soil layers and thermal conductivity in the models (Table S1). Furthermore, the magnitude of warming predictions varied between models by 7°C (Figure 3). Predictions of soil and air warming in Gelisol-dominated regions characterized by tundra ecosystems and permafrost are the most uncertain. This could be related to the uncertainty of polar amplification trends (Bekryaev et al., 2010). Some models represent the dependence of thermal conductivity on organic matter content, advective heat transport by soil water, and latent heat flux in thawing and freezing. These factors may influence the seasonal amplitude of soil temperature with depth, particularly in permafrost regions (Koven & Stern, 2013), and could also lead to some of the variability seen in the warming predictions at high latitudes.

All models agreed on the rapid transfer of shallow soil temperatures to the deep soil stemming from many similarities in the representations of soil heat transport derived from the same underlying land models (CLM and LM3; Table S1), using relationships defined by Dickinson and Kennedy (1993). None of the models appear to represent a significant change in soil thermal conductivity within Gelisol soil where an active layer-permafrost transition could reduce thermal conductivity due to latent heat effects (Figure 3a). However, the degree to which this latent heat effect would impact annual mean soil temperatures is likely minimal.

The failure of some ESMs to recreate the air-soil temperature offset (ΔT_{surf}) measured at observation sites in permafrost regions was apparent in the greater spread in model predictions of soil warming in high-latitude regions. Models that lack distinct snow layers above the soil results in air temperatures more directly impacting the uppermost layer soil temperatures rather than accounting for the insulating effect of snow above the soil surface, leading to their inability to recreate the observed ΔT_{surf} in permafrost areas (Koven & Stern, 2013). This difference in snow representation, along with interactions between temperature, energy, and water exchange at the air-soil interface, leads to less ESM agreement on air-soil temperature offsets in colder and wetter regions of North America (Garcia-Garcia et al., 2019) and other high-latitude regions compared to areas with hotter and drier climates. Failure to capture this quasi steady state ΔT_{surf} likely leads to a misinterpretation of how air warming will impact soil warming in the same areas.

In temperate regions, ΔT_{surf} estimates from the ESMs showed strong agreement; however, those with insulating snow effects, such as bcc-csm1-1, BNU-ESM, CCSM4, CESM1-BGC, GISS-E2-R, inmcm4, MRI-CGCM3, and NorESM1-M, better captured cold forest and grassland observational patterns (Figures 7a and 8a). None of the models appeared to capture the slightly higher ΔT_{surf} seen in the observational data from grassland sites as compared to forested sites (Figures 7a and 8a). Field studies have shown substantial differences in ΔT_{surf} as a result of land cover (Beltrami & Kellman, 2003; Nitou & Beltrami, 2005; Song et al., 2013). Grassland sites tended to have a higher ΔT_{surf} than the forested sites in our observation data set (Figure 7a). This could possibly be due to the effect of trees on shading direct sun exposure of the soil, which can influence surface-soil temperature, or due to the increased surface roughness in forests, which increases sensible heat loss in forests.

The lack of a temperature offset between shallow and deep soils (ΔT_{deep}) across the observation sites further demonstrates the lack of vegetation or land cover effect on heat transport down the soil profile (Figure 7b). This effect was captured well by the ESMs in temperate ecosystems, but not in permafrost (Figure 8b). The negative ΔT_{deep} values of several ESMs including NorESM1-M, CCSM4, GFDL-ESM 2G, inmcm4, and

CESM-BGC could be due to an overestimation of the interseasonal difference in thermal conductivity of organic soils (Koven & Stern, 2013). HadGEM2-ES and IPSL-CM5A-LR overestimate the ΔT_{deep} in permafrost soils, possibly due to their unique structure of their air-soil interface (Koven et al., 2013).

4.4. Influence of Soil Drying

In addition to temperature, soil moisture is also critical for ecosystem function and may affect temperature sensitivity of, for example, soil carbon decomposition (Craine & Gelderman, 2011; Sierra et al., 2015), but projections of soil moisture are much more uncertain. Although the CMIP5 ensemble mean predicted drying across most soil orders, there was considerable variation among model predictions in high-latitude regions (Figure 6). Due to the interactions between soil moisture and sensible heat fluxes, uncertainties in the predictions of soil moisture trends impact soil temperature predictions (Seneviratne et al., 2013). All of the ESMs share processes that link soil hydraulic and thermal properties, including dependence of thermal diffusivity and surface albedo on soil moisture, and evaporation influences on soil temperature. We focus here mainly on temperature predictions and their implications due to this high degree of uncertainty in the long-term trends of soil drying. Moisture is more difficult to predict than soil temperature due to the complex relationships between radiative forcing, temperature, precipitation, and evapotranspiration (Orlowsky & Seneviratne, 2013).

4.5. Implications of Warming Soil Temperatures

Temperature is recognized as a fundamental control on belowground aspects of agricultural production (Egli et al., 2005; FAO, 1985; Huang, 2016; Kaspar & Bland, 1992). Even a few degrees of warming, like that predicted this century, could easily push certain agricultural regions above the optimum temperature ranges for many staple crops where they have historically been grown (FAO, 1985) and have adverse effects on major crop yields (Lobell & Field, 2007; Zhao et al., 2017). Likewise, change in temperatures will alter cold stratification and the timing of seed germination (Walck et al., 2011), the extent of suitable crop climate envelopes (Jarvis et al., 2008; USDA, 1994), and the range of pests and pathogens (Bebber et al., 2013). As the number of days per year with below-freezing soil temperatures, which inhibit seed germination (Boyd & Lemos, 2013; Brown & Blackburn, 1987), decrease or disappear over the 21st century, some regions will become more suitable for agricultural production even as others become less suitable. “Climate smart” agricultural practices, aimed at reducing greenhouse gas emissions, can be adopted to minimize the harmful impacts of warming if accurate predictions of soil warming trends are available (Challinor et al., 2014).

Although the temperature sensitivity of soil decomposers is well documented (Conant et al., 2011; Davidson & Janssens, 2006), global predictions of soil carbon responses to warming air temperatures are highly variable (Todd-Brown et al., 2014; Wu et al., 2018). CMIP5 model predictions of rapid transfer of the warming signal from air to shallow and deep soils, along with a slight lag in air-to-soil warming in snow covered regions, provide more precise soil temperature predictions that can be used to constrain predictions of how decomposition may respond to warming over the coming decades (Schuur et al., 2015). In particular, experimental evidence suggests that the rapid transfer of heat from surface to deep soils shown here will lead to greater soil carbon losses than previously estimated based on surface soil warming only (Hanson et al., 2011; Hicks Pries et al., 2017). Thus, the CMIP5 model predictions demonstrate the regional patterns for the extent to which surface air warming translates to soil warming, which should be considered in valuating temperature sensitive soil processes.

Acknowledgments

This research was supported in part by the U.S. Department of Energy Office of Science, Office of Biological and Environmental Research Terrestrial Ecosystem Science and Regional and Global Model Analysis Programs under, Award DE-SC-0001234. Original data used for this project can be found at <https://esgf-node.llnl.gov/search/cmip5/>. This material is also based upon the work supported by the National Science Foundation under Grant DGE-1450053.

References

- Bebber, D., Ramotowski, M., & Gurr, S. (2013). Crop pests and pathogens move polewards in a warming world. *Nature Climate Change*, 3(11), 985–988.
- Bekryaev, R. V., Polyakov, I. V., & Alexeev, V. A. (2010). Role of polar amplification in long-term surface air temperature variations and modern Arctic warming. *Journal of Climate*, 23(14), 3888–3906. <https://doi.org/10.1175/2010JCLI3297.1>
- Beltrami, H., & Kellman, L. (2003). An examination of short- and long-term air-ground temperature coupling. *Global and Planetary Change*, 38(3–4), 291–303.
- Boyd, C. S., & Lemos, J. A. (2013). Freezing stress influences emergence of germinated perennial grass seeds. *Rangeland Ecology & Management*, 66(2), 136–142.
- Brown, D. M., & Blackburn, W. J. (1987). Impacts of freezing temperatures on crop production in Canada. *Canadian Journal of Plant Science*, 67(4), 1167–1180.
- Challinor, A. J., Watson, J., Lobell, D. B., Howden, S. M., Smith, D. R., & Chhetri, N. (2014). A meta-analysis of crop yield under climate change and adaptation. *Nature Climate Change*, 4(4), 287–291.

- Chen, S. Y., Zhang, X. Y., Pei, D., Sun, H. Y., & Chen, S. L. (2007). Effects of straw mulching on soil temperature, evaporation and yield of winter wheat: Field experiments on the North China Plain. *Annals of Applied Biology*, 150, 261–268.
- Conant, R. T., Ryan, M. G., Ågren, G. I., Birge, H. E., Davidson, E. A., Eliasson, P. E., et al. (2011). Temperature and soil organic matter decomposition rates—Synthesis of current knowledge and a way forward. *Global Change Biology*, 17(11), 3392–3404. <https://doi.org/10.1111/j.1365-2486.2011.02496.x>
- Craine, J. M., & Gelderman, T. M. (2011). Soil moisture controls on temperature sensitivity of soil organic carbon decomposition for a mesic grassland. *Soil Biology and Biochemistry*, 43(2), 455–457.
- Davidson, E., & Janssens, I. (2006). Temperature sensitivity of soil carbon decomposition and feedbacks to climate change. *Nature*, 440(7081), 165–173. <https://doi.org/10.1038/nature04514>
- Decker, K. L. M., Wang, D., Waite, C., & Scherbatskoy, T. (2003). Snow removal and ambient air temperature effects on forest soil temperatures in Northern Vermont. *Soil Science Society of America Journal*, 67(4), 1234–1242. <https://doi.org/10.2136/sssaj2003.1234>
- Dickinson, H.-S., & Kennedy (1993). *Biosphere-atmosphere transfer scheme (BATS) version 1e as coupled to the NCAR Community Climate Model*. NCAR Technical Note. Boulder, Colorado, USA: National Center for Atmospheric Research, CLimate and Global Dynamics Division.
- Egli, D. B., TeKrony, D. M., Heitholt, J. J., & Rupe, J. (2005). Air temperature during seed filling and soybean seed germination and vigor Contribution No. 03-06-129 from the Kentucky Agricultural Experiment Station, Univ. of Kentucky, Lexington, KY 40546-0312. *Crop Science*, 45(4), 1329–1335. <https://doi.org/10.2135/cropsci2004.0029>
- FAO (1985). Agronomic factors. In *Guidelines: Land evaluation for irrigated agriculture—FAO soils bulletin 55*. Rome, Italy: Food and Agriculture Organization of the United Nations.
- FAO-UNESCO, & USDA-NRCS. (2005). Global soil regions map. https://www.nrcs.usda.gov/wps/portal/nrcs/detail/soils/use/?cid=nrcs142p2_054013.
- García-García, A., Cuesta-Valero, F. J., Beltrami, H., & Smerdon, J. E. (2019). Characterization of air and ground temperature relationships within the CMIP5 historical and future climate simulations. *Journal of Geophysical Research: Atmospheres*, 124(7), 3903–3929.
- García-Suárez, A. M., & Butler, C. J. (2006). Soil temperatures at Armagh Observatory, Northern Ireland, from 1904 to 2002. *International Journal of Climatology*, 26(8), 1075–1089.
- Hanson, P. J., Childs, K. W., Wullschleger, S. D., Riggs, J. S., Thomas, W. K., Todd, D. E., & Warren, J. M. (2011). A method for experimental heating of intact soil profiles for application to climate change experiments: Experimental heating of intact soil profiles. *Global Change Biology*, 17(2), 1083–1096.
- Hao, G., Zhuang, Q., Pan, J., Jin, Z., Zhu, X., & Liu, S. (2014). Soil thermal dynamics of terrestrial ecosystems of the conterminous United States from 1948 to 2008: An analysis with a process-based soil physical model and AmeriFlux data. *Climate Change*, 126(1-2), 135–150.
- Hatfield, J. L., Boote, K. J., Kimball, B. A., Ziska, L. H., Izaurralde, R. C., Ort, D., et al. (2011). Climate impacts on agriculture: Implications for crop production. *Agronomy Journal*, 103(2), 351–370. <https://doi.org/10.2134/agronj2010.0303>
- Holland, M.M. and Bitz, C.M. (2003). Polar amplification of climate change in coupled models. *Climate Dynamics*, 21(3), 221–232. journal article. <https://doi.org/10.1007/s00382-003-0332-6>
- Hu, Q., and Feng, S. (2003). A daily soil temperature dataset and soil temperature climatology of the contiguous United States. *Journal of Applied Meteorology*, 42(8), 1139–1156. <https://journals.ametsoc.org/doi/abs/10.1175/1520-0450%282003%29042%3C1139%3AADSTD%3E2.0.CO%3B2>
- Huang, J. (2016). Effects of soil temperature and snow cover on the mortality of overwintering pupae of the cotton bollworm, *Helicoverpa armigera* (Hübner) (Lepidoptera: Noctuidae). *International Journal of Biometeorology*, 60(7), 977–989. journal article. <https://doi.org/10.1007/s00484-015-1090-y>
- Jarvis, A., Lane, A., & Hijmans, R. J. (2008). The effect of climate change on crop wild relatives. *Agriculture Ecosystems & Environment*, 126, 13–23.
- Jenny, H. (1941). *Factors of soil formation: A system of quantitative pedology*. New York: McGraw-Hill.
- Jobbágy, E.G. and Jackson, R.B. (2001). The distribution of soil nutrients with depth: Global patterns and the imprint of plants. *Biogeochemistry*, 53(1), 51–77. journal article. <https://doi.org/10.1023/A:1010760720215>
- Jungqvist, G., Oni, S. K., Teutschbein, C., & Futter, M. N. (2014). Effect of climate change on soil temperature in Swedish boreal forests. *Plos One*, 9(4), e93957. <https://doi.org/10.1371/journal.pone.0093957>
- Kaspar, T. C., & Bland, W. L. (1992). Soil temperature and root growth. *Soil Science*, 154(4), 290–299. https://journals.lww.com/soilsci/Fulltext/1992/10000/SOIL_TEMPERATURE_AND_ROOT_GROWTH.5.aspx
- Koch, Tscherko, & Kandeler. (2007). Temperature sensitivity of microbial respiration, nitrogen mineralization, and potential soil enzyme activities in organic alpine soils. *Global Biogeochemical Cycles*, 21(4). <https://agupubs.onlinelibrary.wiley.com/doi/abs/10.1029/2007GB002983>
- Koven, C.D., Ringeval, B., Friedlingstein, P., Ciais, P., Cadule, P., Khvorostyanov, D., et al. (2011). Permafrost carbon-climate feedbacks accelerate global warming. *Proceedings of the National Academy of Sciences*, 108(36), 14,769–14,774. <https://www.pnas.org/content/prnas/108/36/14769.full.pdf>
- Koven, R., & Stern (2013). Analysis of permafrost thermal dynamics and response to climate change in the CMIP5 Earth system models. *Journal of Climate*, 26(6), 1877–1900.
- Krasting, J. P., Broccoli, A. J., Dixon, K. W., & Lanzante, J. R. (2013). Future changes in Northern Hemisphere snowfall. *Journal of Climate*, 26(20), 7813–7828. <https://journals.ametsoc.org/doi/abs/10.1175/JCLI-D-12-00832.1>
- Lawrence, D. M., Oleson, K. W., Flanner, M. G., Thornton, P. E., Swenson, S. C., Lawrence, P. J., et al. (2011). Parameterization improvements and functional and structural advances in Version 4 of the Community Land Model. *J. Adv. Model. Earth Syst.*, 3(3).
- Lesperance, M., Smerdon, J. E., & Beltrami, H. (2010). Propagation of linear surface air temperature trends into the terrestrial subsurface. *Journal of Geophysical Research: Atmospheres*, 115(D21). <https://agupubs.onlinelibrary.wiley.com/doi/abs/10.1029/2010JD014377>
- Lloyd, J., & Taylor, J. A. (1994). On the temperature dependence of soil respiration. *Functional Ecology*, 8(3), 315–323.
- Lobell, D. B., & Field, C. B. (2007). Global scale climate-crop yield relationships and the impacts of recent warming. *Environmental Research Letters*, 2(014002), 1–7.
- Maurer, G. E., & Bowling, D. R. (2014). Seasonal snowpack characteristics influence soil temperature and water content at multiple scales in interior western U.S. mountain ecosystems. *Water Resour. Res.*, 50, 5216–5234.
- Mohler, R. L., & Harrington, J. (2012). Differences in Kansas soil temperatures between the 1990s and 2000s. *Trans. Kans. Acad. Sci.*, 115(3-4), 167–175.
- Nitoiu, D., & Beltrami, H. (2005). Subsurface thermal effects of land use changes. *J. Geophys. Res.*, 110(F1).

- Ochsner, T. E., Horton, R., & Ren, T. (2000). A new perspective on soil thermal properties. *Soil Science Society of America Journal*, 65(6), 1641–1647.
- Oechel, W. C., Hastings, S. J., Vourlirtis, G., Jenkins, M., Riechers, G., & Grulke, N. (1993). Recent change of Arctic tundra ecosystems from a net carbon dioxide sink to a source. *Nature*, 361, 520–523.
- Orlowsky, B., & Seneviratne, S. I. (2013). Elusive drought: Uncertainty in observed trends and short- and long-term CMIP5 projections. *Hydrology and Earth System Sciences*, 17(1765–1781).
- Pries, C. E. H., Castanha, C., Porras, R. C., & Torn, M. S. (2017). The whole-soil carbon flux in response to warming. *Science*, 355(6332), 1420–1423.
- Schmidt, M. W., Torn, M. S., Abiven, S., Dittmar, T., Guggenberger, G., Janssens, I. A., et al. (2011). Persistence of soil organic matter as an ecosystem property. *Nature*, 478(7367), 49–56. Article. <Go to ISI>://WOS:000295575400033
- Schmidt, W. L., Gosnold, W. D., & Enz, J. W. (2001). A decade of air-ground temperature exchange from Fargo, North Dakota. *Global and Planetary Change*, 29, 311–325.
- Schuur, E. A. G., McGuire, A. D., Schädel, C., Grosse, G., Harden, J. W., Hayes, D. J., et al. (2015). Climate change and the permafrost carbon feedback. *Nature*, 520(7546), 171–179. <https://www.ncbi.nlm.nih.gov/pubmed/25855454>, <https://doi.org/10.1038/nature14338>
- Seneviratne, S. I., Wilhelm, M., Stanelle, T., van den Hurk, B., Hagemann, S., Berg, A., et al. (2013). Impact of soil moisture-climate feedbacks on CMIP5 projections: First results from the GLACE-CMIP5 experiment. *Geophysical Research Letters*, 40(19), 5212–5217.
- Shufen, S. and Xia, Z. (2004). Effect of the lower boundary position of the Fourier equation on the soil energy balance. *Advances in Atmospheric Sciences*, 21(6), 868–878. journal article. <https://doi.org/10.1007/BF02915589>
- Sierra, C. A., Trumbore, S. E., Davidson, E. A., Vicca, S., & Janssens, I. (2015). Sensitivity of decomposition rates of soil organic matter with respect to simultaneous changes in temperature and moisture. *Journal of Advances in Modeling Earth Systems*, 07.
- Šimůnek, J., Šejna, M., Saito, H., Sakai, M., & van Genuchten, M. T. (2013). *The Hydrus-1D software package for simulating the movement of water, heat, and multiple solutes in variably saturated media, Version 4.17*. Riverside, California, USA: Dept of Environmental Sciences, University of California.
- Slater, A. G., & Lawrence, D. M. (2013). Diagnosing present and future permafrost from climate models. *Journal of Climate*, 26(15), 5608–5623.
- Smerdon, J. E., Pollack, H. N., Cermak, V., Enz, J. W., Kresl, M., Safanda, J., & Wehmiller, J. F. (2004). Air-ground temperature coupling and subsurface propagation of annual temperature signals. *J. Geophys. Res.*, 109.
- Smerdon, J. E., Pollack, H. N., Enz, J. W., & Lewis, M. J. (2003). Conduction-dominated heat transport of the annual temperature signal in soil. *Journal of Geophysical Research: Solid Earth*, 108(B9). <https://agupubs.onlinelibrary.wiley.com/doi/abs/10.1029/2002JB002351>
- Smerdon, J. E., & Stieglitz, M. (2006). Simulating heat transport of harmonic temperature signals in the Earth's shallow subsurface: Lower-boundary sensitivities. *Geophysical Research Letters*, 33(14). <https://agupubs.onlinelibrary.wiley.com/doi/abs/10.1029/2006GL026816>
- Sokratov, S. A., & Barry, R. G. (2002). Intraprofessional variation in the thermoinsulation effect of snow cover on soil temperatures and energy balance. *Journal of Geophysical Research*, 107(D10), 4093.
- Song, Y., Zhou, D., Zhang, H., Li, G., Jin, Y., & Li, Q. (2013). Effects of vegetation height and density on soil temperature variations. *Chin. Sci. Bull.*, 58(8), 907–912.
- Taylor, K. E., Stouffer, R. J., & Meehl, G. A. (2012). An overview of CMIP5 and the experiment design. *Bulletin of the American Meteorological Society*, 93, 485–498.
- Todd-Brown, K. E. O., Randerson, J. T., Hopkins, F., Arora, V., Hajima, T., Jones, C., et al. (2014). Changes in soil organic carbon storage predicted by Earth system models during the 21st century. *Biogeosciences*, 11(8), 2341–2356. <Go to ISI>://WOS:000335374200016
- USDA (1994). *Major world crop areas and climatic profiles*. World Agricultural Outlook Board, Agricultural Handbook No. 664. Washington, DC: USDA.
- Van Vuuren, D. P., Edmonds, J., Kainuma, M., Riahi, K., Thomson, A., Hibbard, K., et al. (2011). The representative concentration pathways: An overview. *Climate Change*, 109(1–2), 5–31.
- Walck, J. L., Hidayati, S. N., Dixon, K. W., Thompson, K. E. N., & Poschlod, P. (2011). Climate change and plant regeneration from seed. *Global Change Biology*, 17(6), 2145–2161.
- Wraith, J. M., & Ferguson, A. H. (1994). Soil temperature limitation to water use by field-grown winter wheat. *Agronomy Journal*, 86(6), 974–979. <https://doi.org/10.2134/agronj1994.00021962008600060009>
- Wu, D., Piao, S., Liu, Y., Ciais, P., & Yao, Y. (2018). Evaluation of CMIP5 Earth system models for the spatial patterns of biomass and soil carbon turnover times and their linkage with climate. *Journal of Climate*, 31(15), 5947–5960. <https://journals.ametsoc.org/doi/abs/10.1175/JCLI-D-17-0380.1>
- Zender, C. S. (2008). Analysis of self-describing gridded geoscience data with netCDF operators (NCO). *Environmental Modelling Software*, 23(10), 1338–1342.
- Zhang, N., & Wang, Z. (2017). Review of soil thermal conductivity and predictive models. *International Journal of Thermal Sciences*, 117, 172–183.
- Zhang, T. (2005). Influence of the seasonal snow cover on the ground thermal regime: An overview. *Rev. Geophys.*, 43.
- Zhang, T., Barry, R. G., Gilichinsky, D., Bykhovets, S. S., Sorokovikov, V. A., & Ye, J. (2001). An amplified signal of climatic change in soil temperatures during the last century at Irkutsk. *Russia. Clim. Change*, 49, 41–76.
- Zhang, Y., Chen, W., Smith, S. L., Riseborough, D. W., & Cihlar, J. (2005). Soil temperature in Canada during the twentieth century: Complex responses to atmospheric climate change. *Journal of Geophysical Research: Atmospheres*, 110(D3). <https://agupubs.onlinelibrary.wiley.com/doi/abs/10.1029/2004JD004910>
- Zhao, C., Liu, B., Piao, S., Wang, X., Lobell, D. B., Huang, Y., et al. (2017). Temperature increase reduces global yields of major crops in four independent estimates. *Proceedings of the National Academy of Sciences*, 114(35), 9326–9331. <https://www.pnas.org/content/pnas/114/35/9326.full.pdf>